

## Rational Design of Bimetallic Alloys for Effective Hydrodechlorination of 4-Chlorophenol

Chaitra S. Shenoy<sup>a</sup>, Shelaka Gupta<sup>b\*</sup>, M. Ali Haider<sup>a\*</sup>, Tuhin S. Khan<sup>c\*</sup>

<sup>a</sup>Renewable Energy and Chemicals Laboratory, Department of Chemical Engineering, Indian Institute of Technology Delhi, Hauz Khas, New Delhi 110016, India

<sup>b</sup>Department of Chemical Engineering, Indian Institute of Technology Hyderabad, Kandi, Sangareddy, Telangana 502285, India

<sup>c</sup>Light Stock Processing Division, CSIR – Indian Institute of Petroleum, Mohkampur, Dehradun 248005, India

Corresponding Authors: Shelaka Gupta (shelaka@che.iith.ac.in), M. Ali Haider (haider@iitd.ac.in), Tuhin S. Khan (tuhins.khan@iip.res.in)

Table 1. The d-band centers of Pd and Pd-based alloys

Surface	d-band center
Pd (111)	-1.67 eV
Pd <sub>3</sub> Cu (111)	-1.12 eV
Pd <sub>3</sub> Ag (111)	-1.73 eV
Pd <sub>3</sub> Au (111)	-1.77 eV

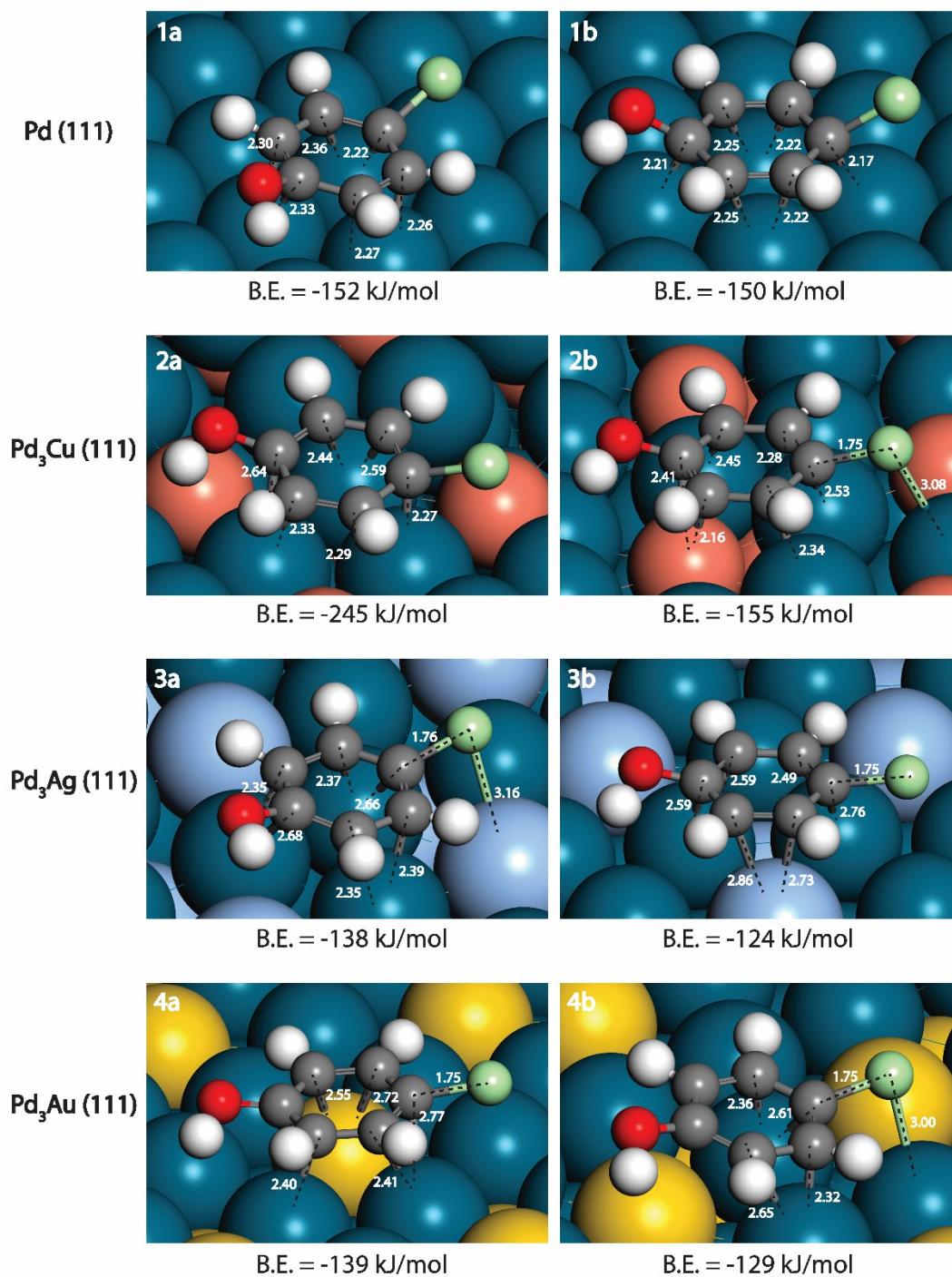


Figure S1(A). Various Binding Modes of 4-CP on (1) Pd (111), (2) Pd<sub>3</sub>Cu (111), (3) Pd<sub>3</sub>Ag (111) and (4) Pd<sub>3</sub>Au (111) surfaces.

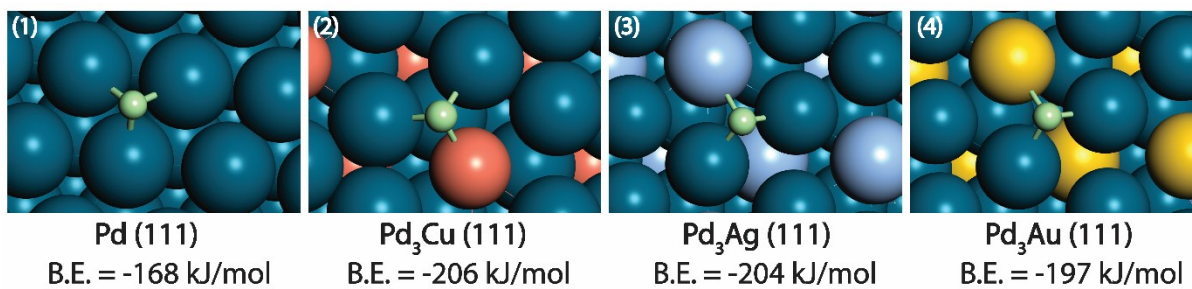


Figure S1(B). The Most Stable Binding Modes of Cl on (1) Pd (111), (2) Pd<sub>3</sub>Cu (111), (3) Pd<sub>3</sub>Ag (111) and (4) Pd<sub>3</sub>Au (111) surfaces.

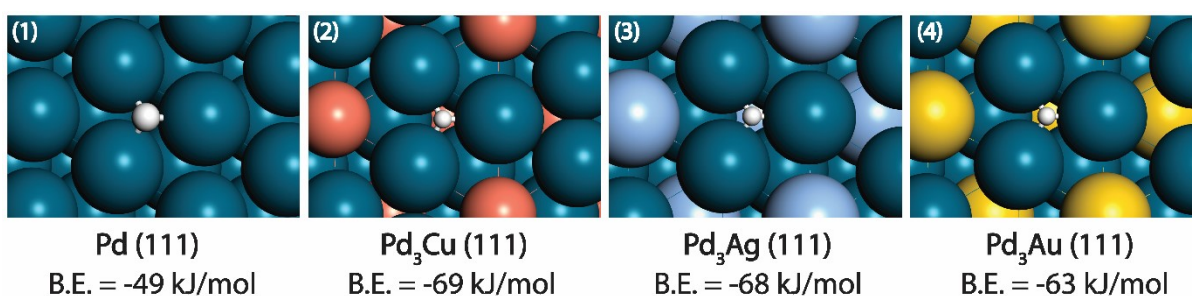


Figure S1(C). The Most Stable Binding Modes of H on (1) Pd (111), (2) Pd<sub>3</sub>Cu (111), (3) Pd<sub>3</sub>Ag (111) and (4) Pd<sub>3</sub>Au (111) surfaces.

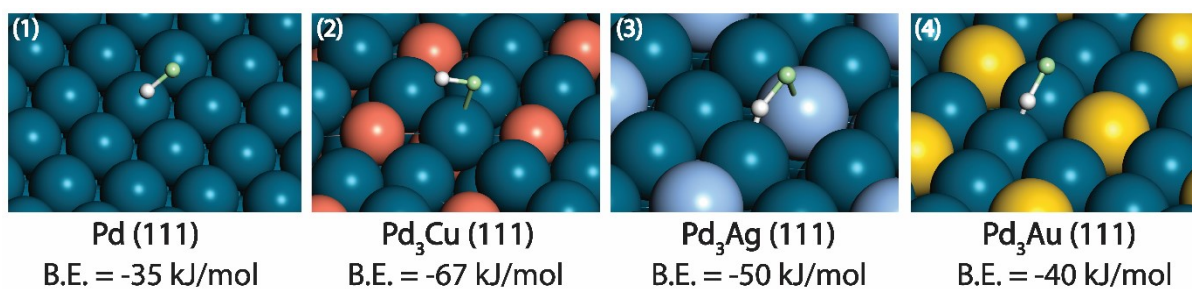


Figure S1(D). The Most Stable Binding Modes of HCl on (1) Pd (111), (2) Pd<sub>3</sub>Cu (111), (3) Pd<sub>3</sub>Ag (111) and (4) Pd<sub>3</sub>Au (111) surfaces.

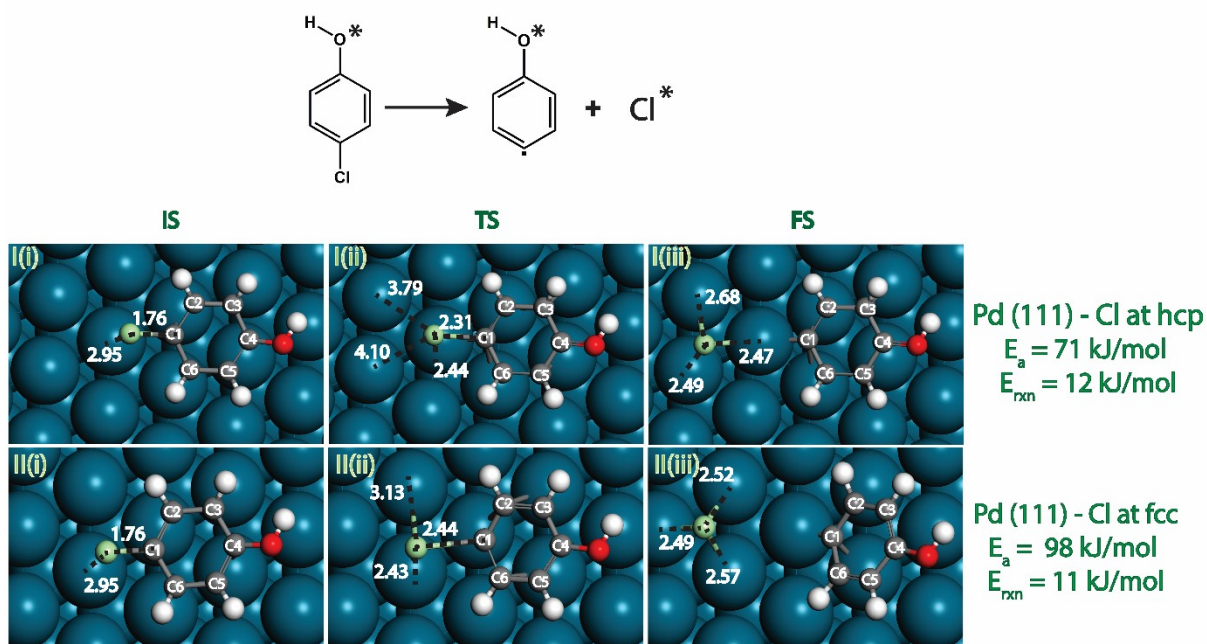
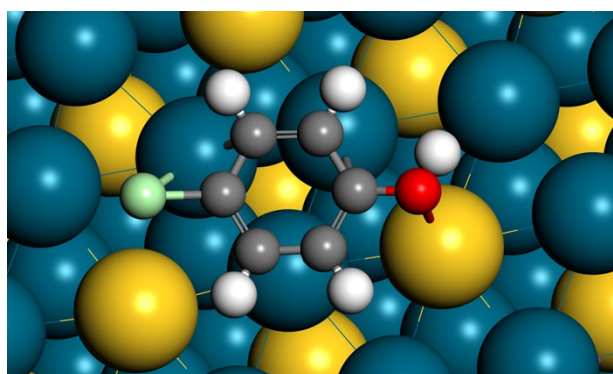


Figure S2. Transition state structures on the Pd (111) surface for the C-Cl bond dissociation step with Cl at the hcp site (I) and Cl at the fcc site (II).



B.E = -128 kJ/mol

Figure S3. Binding Energy of 4-CP over the fcc site on the Pd<sub>3</sub>Au (111) surface.



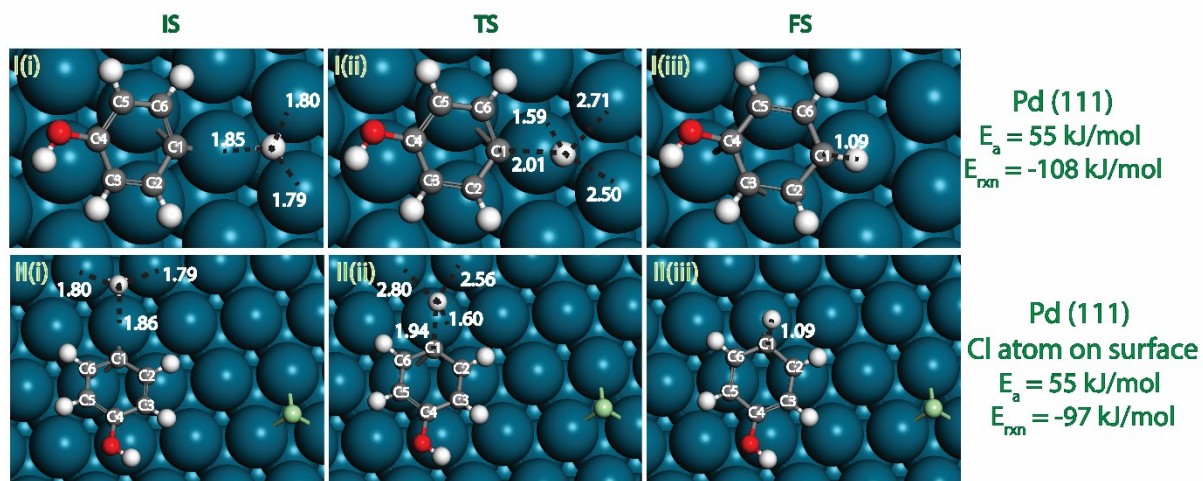
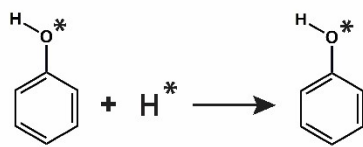


Figure S4. Transition state structures for the hydrogenation step to form phenol without Cl on the surface (I) and with Cl at the fcc site (II).

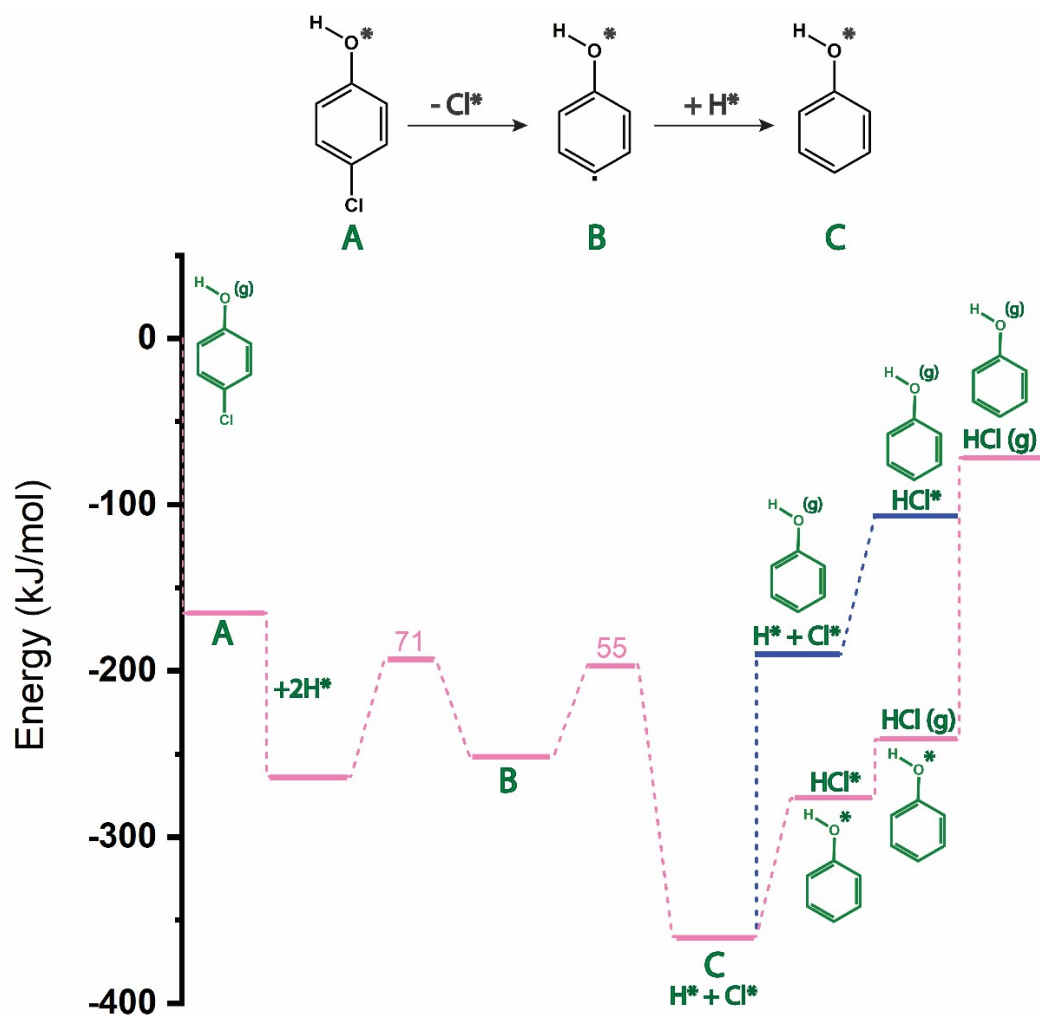
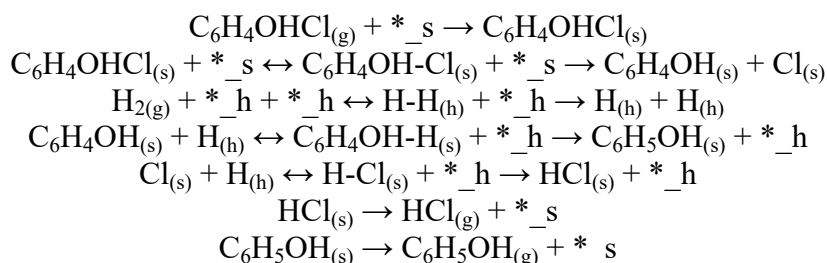


Figure S5. Energy Diagram for the HDC of 4-CP over the Pd (111) surface (the pathway for phenol desorption followed by HCl desorption is displayed in blue and the pathway for HCl desorption followed by phenol desorption is displayed in pink).

In order to understand the HDC of 4-CP over the different surfaces (Pd (111), Pd<sub>3</sub>Cu (111), Pd<sub>3</sub>Ag (111) and Pd<sub>3</sub>Au (111)), a set of elementary steps are solved simultaneously as described in the Methodology Section. The elementary steps are given below:



where,

\*<sub>-s</sub> denotes free surface site

\*<sub>-h</sub> denotes free hydrogen site

Subscripts (g), (s) and (h) denotes gas phase species, surface species and hydrogen occupied surface site

→ denotes the product species formation step

↔ denotes the transition state species formation

Due to the small size of the hydrogen atom, a separate reservoir is assigned for hydrogen, denoted by (h), as it would not compete with other intermediates for adsorption sites, denoted by (s). The hydrogen reservoir model has been used by Prof. Norskov and co-workers<sup>1</sup> and in our previous publications<sup>2</sup>.

Table 2. Formation Energies of the Species used to Construct the MKM (Reference states considered are CH<sub>4</sub>, H<sub>2</sub>, H<sub>2</sub>O and Cl<sub>2</sub>)

Species	Facet	Surface	Formation Energy (eV)
CH <sub>4</sub>	Gas	None	0.0
H <sub>2</sub>	Gas	None	0.0
H <sub>2</sub> O	Gas	None	0.0
Cl <sub>2</sub>	Gas	None	0.0
C <sub>6</sub> H <sub>4</sub> OHCl	Gas	None	7.34
C <sub>6</sub> H <sub>5</sub> OH	Gas	None	7.53
HCl	Gas	None	-0.93
C <sub>6</sub> H <sub>4</sub> OHCl	111	Pd	5.63
C <sub>6</sub> H <sub>4</sub> OHCl	111	Pd <sub>3</sub> Cu	4.68
C <sub>6</sub> H <sub>4</sub> OHCl	111	Pd <sub>3</sub> Ag	5.78
C <sub>6</sub> H <sub>4</sub> OHCl	111	Pd <sub>3</sub> Au	5.77

C <sub>6</sub> H <sub>4</sub> OH	111	Pd	7.41
C <sub>6</sub> H <sub>4</sub> OH	111	Pd <sub>3</sub> Cu	6.46
C <sub>6</sub> H <sub>4</sub> OH	111	Pd <sub>3</sub> Ag	7.37
C <sub>6</sub> H <sub>4</sub> OH	111	Pd <sub>3</sub> Au	7.23
C <sub>6</sub> H <sub>5</sub> OH	111	Pd	5.77
C <sub>6</sub> H <sub>5</sub> OH	111	Pd <sub>3</sub> Cu	5.82
C <sub>6</sub> H <sub>5</sub> OH	111	Pd <sub>3</sub> Ag	6.16
C <sub>6</sub> H <sub>5</sub> OH	111	Pd <sub>3</sub> Au	6.11
H	111	Pd	-0.51
H	111	Pd <sub>3</sub> Cu	-0.71
H	111	Pd <sub>3</sub> Ag	-0.69
H	111	Pd <sub>3</sub> Au	-0.66
Cl	111	Pd	-1.65
Cl	111	Pd <sub>3</sub> Cu	-2.14
Cl	111	Pd <sub>3</sub> Ag	-2.12
Cl	111	Pd <sub>3</sub> Au	-2.04
HCl	111	Pd	-1.34
HCl	111	Pd <sub>3</sub> Cu	-2.66
HCl	111	Pd <sub>3</sub> Ag	-1.45
HCl	111	Pd <sub>3</sub> Au	-1.35
C <sub>6</sub> H <sub>4</sub> OH-Cl	111	Pd	6.37
C <sub>6</sub> H <sub>4</sub> OH-Cl	111	Pd <sub>3</sub> Cu	5.47
C <sub>6</sub> H <sub>4</sub> OH-Cl	111	Pd <sub>3</sub> Ag	6.24
C <sub>6</sub> H <sub>4</sub> OH-Cl	111	Pd <sub>3</sub> Au	6.46
C <sub>6</sub> H <sub>4</sub> OH-H	111	Pd	7.56
C <sub>6</sub> H <sub>4</sub> OH-H	111	Pd <sub>3</sub> Cu	6.56
C <sub>6</sub> H <sub>4</sub> OH-H	111	Pd <sub>3</sub> Ag	7.44
C <sub>6</sub> H <sub>4</sub> OH-H	111	Pd <sub>3</sub> Au	7.72
H-H	111	Pd	0.12
H-H	111	Pd <sub>3</sub> Cu	-0.43
H-H	111	Pd <sub>3</sub> Ag	0.02
H-H	111	Pd <sub>3</sub> Au	-0.27
H-Cl	111	Pd	-1.21
H-Cl	111	Pd <sub>3</sub> Cu	-2.66
H-Cl	111	Pd <sub>3</sub> Ag	-1.39
H-Cl	111	Pd <sub>3</sub> Au	-1.31



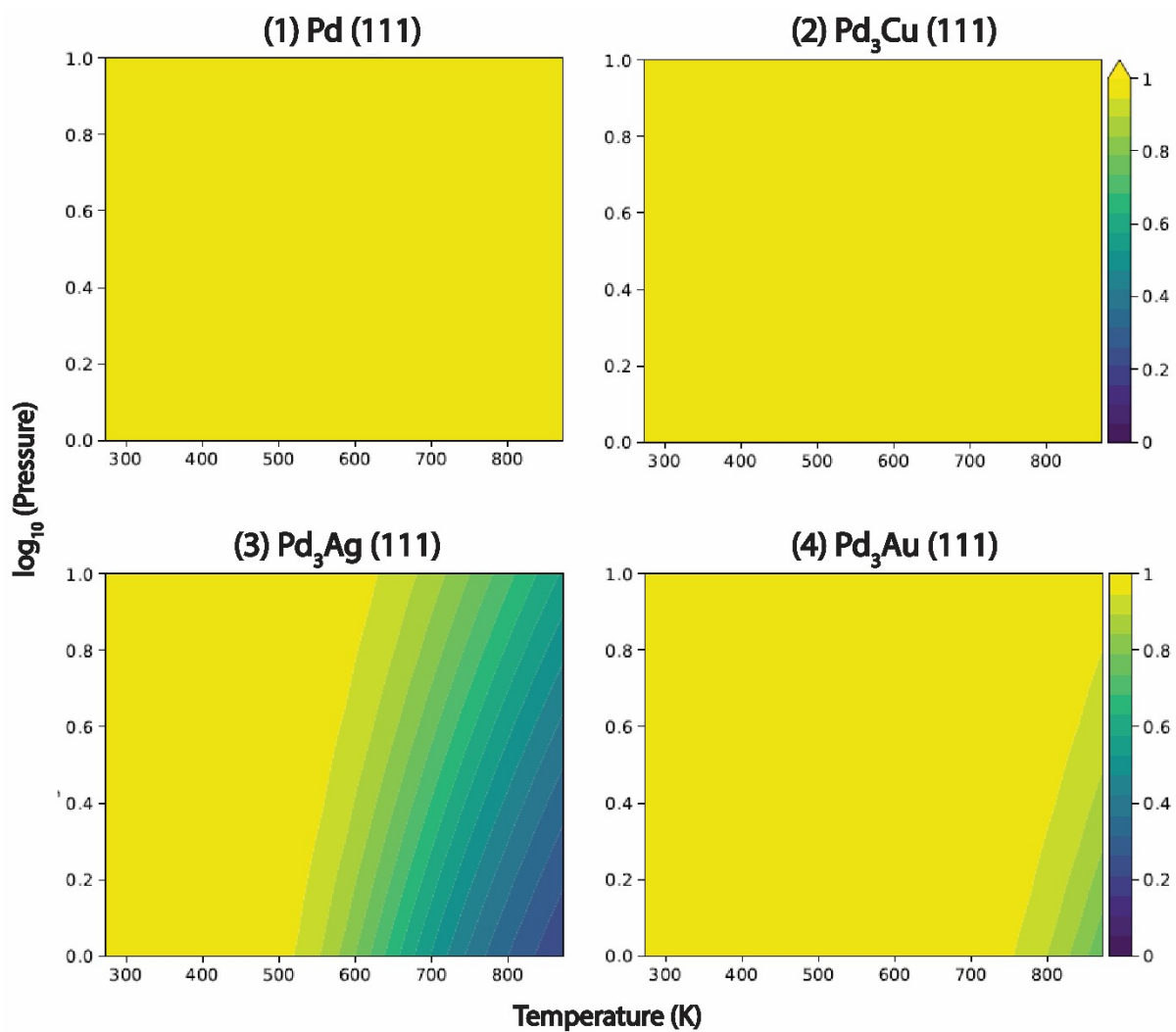


Figure S6. Surface coverage of  $\text{C}_6\text{H}_4\text{OHCl}$  with varying temperatures and pressures over different surfaces ((1) Pd (111), (2) Pd<sub>3</sub>Cu (111), (3) Pd<sub>3</sub>Ag (111) and (4) Pd<sub>3</sub>Au (111))

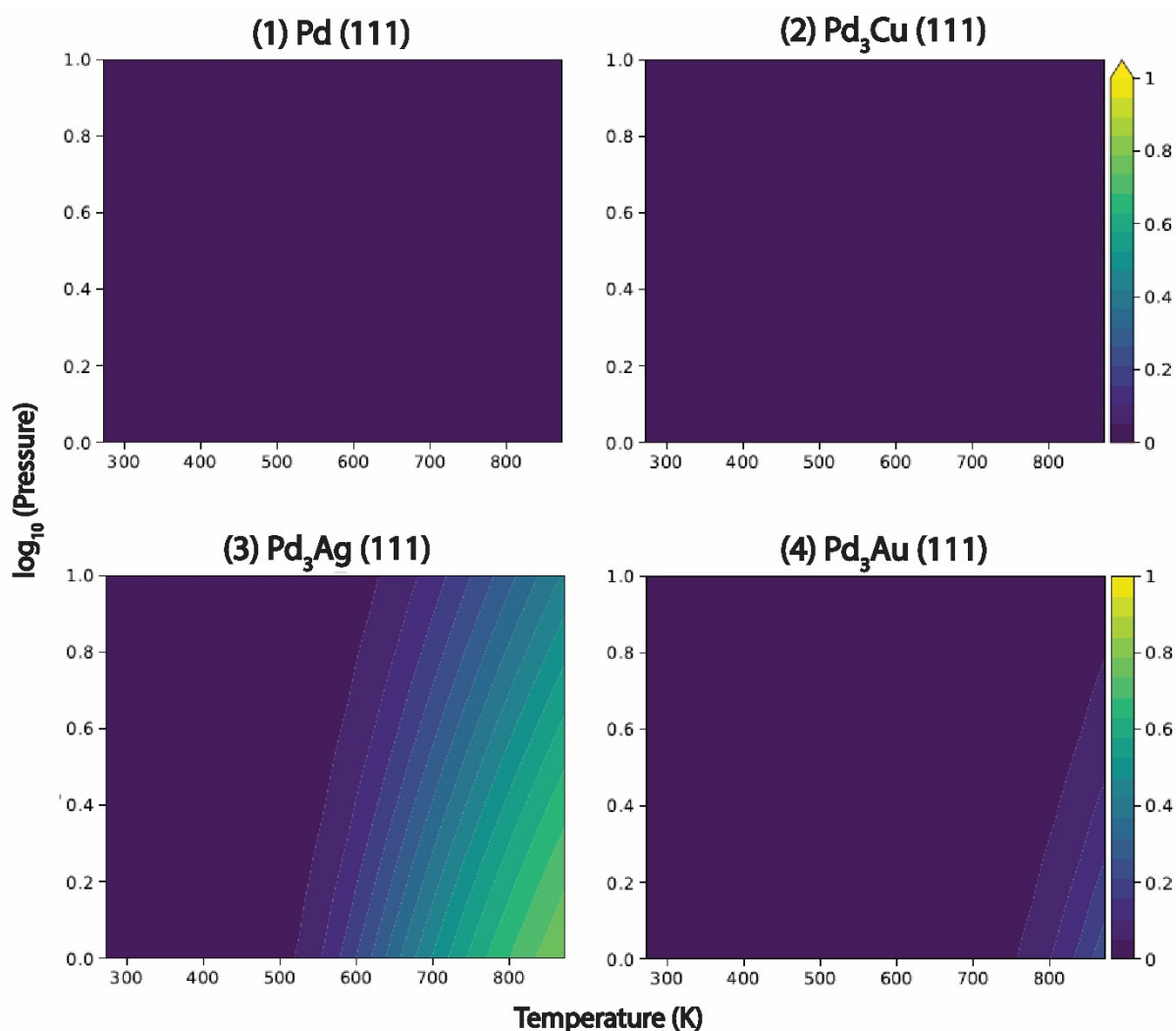


Figure S7. Surface coverage of Cl with varying temperatures and pressures over different surfaces ((1) Pd (111), (2) Pd<sub>3</sub>Cu (111), (3) Pd<sub>3</sub>Ag (111) and (4) Pd<sub>3</sub>Au (111))

## References:

- (1) Medford, A. J.; Lausche, A. C.; Abild-Pedersen, F.; Temel, B.; Schjødt, N. C.; Nørskov, J. K.; Studt, F. Activity and Selectivity Trends in Synthesis Gas Conversion to Higher Alcohols. *Top. Catal.* **2014**, *57* (1–4), 135–142. <https://doi.org/10.1007/s11244-013-0169-0>.
- (2) Jalid, F.; Khan, T. S.; Haider, M. A. CO<sub>2</sub> Reduction and Ethane Dehydrogenation on Transition Metal Catalysts: Mechanistic Insights, Reactivity Trends and Rational Design of Bimetallic Alloys. *Catal. Sci. Technol.* **2021**, *11*, 97–115. <https://doi.org/10.1039/d0cy01290d>.